Science and Technology for Energy Transition **79**, 32 (2024)

https://doi.org/10.2516/stet/2024027

Available online at:
stet-review.org

Decarbonizing Energy Systems: Smart Grid and Renewable Technologies
Fang Rui-ming and Qiangqiang Liao (Guest Editors)

REGULAR ARTICLE OPEN ACCESS

Novel multi-port converter for distributed MPPT operation in solar PV system

NSD Prakash Korlepara[1,*], EB Elanchezhian[2], S Pragaspathy[3], and S Subramanian[2]

[1] Department of Electrical Engineering, Annamalai University, Chidambaram 608002, Tamil Nadu, India
[2] Department of Electrical Engineering, FEAT, Annamalai University, Chidambaram 608002, Tamil Nadu, India
[3] Department of Electrical and Electronics Engineering, Vishnu Institute of Technology, Bhimavaram 534202, Andhra Pradesh, India

Received: 11 January 2024 / Accepted: 11 April 2024

Abstract. Solar photovoltaic (PV) systems continue to be the most prevalent renewable energy resource despite the presence of numerous limitations. A power discrepancy between PV modules on a large scale may result in power dissipation throughout the entire PV system. This particular paper proposes an efficient multi-port converter for distributed maximum power point tracking operation (D-MPPT) for a solar PV system. The operation details of the proposed multi-port converter along with analytical waveforms are presented in this paper. To implement the D-MPPT approach in the proposed multi-port converter, a detailed analysis of mathematical modeling of solar PV systems with a mismatch of PV power and voltage stabilization approach is done. In addition, the proposed approach eliminates the need for additional current sensors and semiconductor components to overcome the effect of mismatched power in the PV system. To validate this, the prototype has been built and integrated with the real environment of the solar PV system. To verify the operation, a detailed simulation study and experimental investigation have been carried out and presented in this paper which reveals that the proposed system offers 24% improved power extraction compared to the centralized converter and MPPT method under partially shaded conditions. After a detailed investigation and discussion of measured results and analysis, it is concluded that the proposed multi-port DC-DC converter is the most suitable solution for solar PV applications.

Keywords: Multi-port DC-DC converter, Photovoltaic systems, D-MPPT, Differential power processing.

1 Introduction

Solar photovoltaic (PV) is one of the most promising energy generation resources due to its pollution-free, friendly environment and standby mode of operation [1, 2]. The global energy market has expanded drastically with the implementation of solar PV on a large scale and helps to achieve social development [3–11]. Partial shading, caused by factors such as the shadows cast by structures like trees, buildings, and poles, as well as the motion of clouds in the case of large-scale PV systems [12, 13], significantly diminishes the power produced by the PV array. The P-V curve has several peaks due to partial shading, which results from nonuniform irradiation conditions and leads to output power losses [14]. Among the most effective parameters on these losses are the shading pattern, position of shaded modules, and array arrangement. In any large-scale solar power plant or solar rooftop system, it is impossible to perform regular maintenance and a unified cleaning approach, thereby leading to a mismatch of power generation and resulting in huge financial losses in power generation [15, 16].

Numerous research works addressed the phenomena of mismatch in PV and its effects on solar PV generation. The research report says that less than 10% of the shading effect on solar PV reduces power generation by up to 70% [17]. Moreover, the mismatch of solar power and internal hotspots severely affects the reliability of solar cells. When a few cells get affected due to the above issues, uneven aging appears on the PV plant. The power generation gets deviated up to 15% beyond 25 years due to this uneven aging [18–20]. In [21], the combined effect of partial shading, poor soiling, non-unified cleaning, and uneven aging effects, creates a large temperature difference inside the PV plant. Further, it aggregates the mismatch of power in solar PV. Maximum power point tracking operation (MPPT) methods are vital in PV systems since the MPP of a solar panel

* Corresponding author: prakash205k@gmail.com

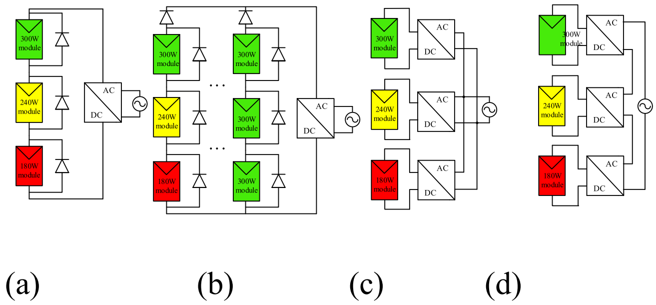

Fig. 1. Solar PV power structure. a) String arrangement PV system; b) array arrangement PV system; c) string-inverter arrangement PV system; d) PV optimizer arrangement [33].

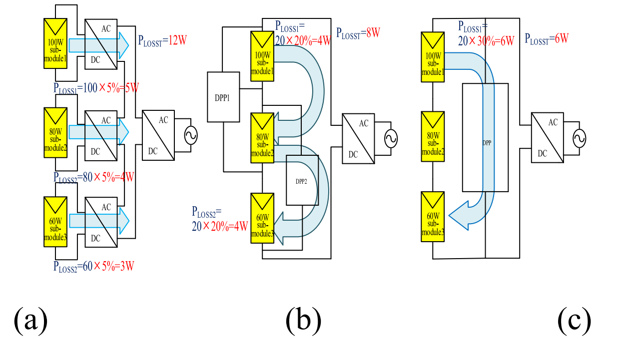

Fig. 2. Loss analyser for solar PV. a) PV optimizer; b) DPP-fed system; c) DPP-fed parallel system.

fluctuates with irradiance and temperature, hence the usage of MPPT algorithms in order to acquire the maximum power from a solar array.

The MPPT operation also fails often due to the presence of multiple local peaks to a mismatch in the PV voltage and power [22]. Conventional MPPT operation fails often by tracking the local peak instead of the actual peak.

From the detailed peer research report, it is understood that mismatches in the PV power cause several issues in the generation losses and other associated problems [23]. To eliminate this particular effect, researchers have proposed many different solutions. In [24] researcher analysed deep learning and quantile regression models for estimating PV power loss due to partial shading for subsequent decisions and dealing with risks. In [25, 26], the reconfiguration of solar PV and the architecture of solar PV are altered to avoid the mismatch. Also, the differential power processing (DPP) approach is presented to neutralize the effect of mismatch and trap the energy under mismatching conditions. Figures 1a and 1b are effective solutions to bypass the current path during mismatch conditions by providing a blocking diode at every PV module. By this approach, the impedance loading can be avoided, thereby hotspots can be eliminated, enabling the safe protection of PV cells. Moreover, this method is a simpler and cost-effective solution to neutralize the effect. The producers incorporate both bypass and blocking diodes as shown in Figures 1a and 1b to ensure safety, dependability, and seamless functioning. The purpose of a bypass diode within a solar panel is to shield an array of partially shaded photovoltaic cells from the normally operating photovoltaic string during the panel's optimum sunlight. The current from the solar panels passes (forward-biased) to the battery and stops (reverse-biased) from the battery to the solar panel because the blocking diode only allows current to travel in one way.

Therefore, the overall energy trapped gets severely affected [27]. To capture these energies and enhance the overall performance of solar PV systems, the distributed MPPT has been proposed by researchers [28–32]. A D-MPPT design reduces the number of MPPs in a PV array by dividing it into smaller arrays, or sub-arrays. Afterwards, a DC/DC power converter is utilised, which employs an MPPT method that is significantly less complex than that of traditional MPPT systems, and each sub-array is coupled to it.

There are two ways to configure the solar PV array before injecting the power into the grid. Figures 1c and 1d are the independent inverter and cascaded inverter structures, respectively to improve the performance in different aspects [28]. The power trapped is not high and mismatches in the sub-modules exist, thereby overall generation gets affected in an independent inverter structure. In a cascaded structure, it achieves local MPPT at each module and enhances the performance. However, due to the presence of a circulation current in each stage of the inverter, the control signal generation is complex [29]. To avoid this circulation path, a DC optimizer can be utilized as shown in Figure 2a. However, it increases the cost of the solar PV system and is complex to control. To solve this issue, the DPP approach is a suitable system and a few articles are published with two-port converters as shown in Figures 2b and 2c. DPP for PV applications has gained significant attention recently due to its substantial improvements over conventional solutions in terms of efficiency, reliability, and cost.

DPP converters are power converters that transmit power within nearby modules or among a string and modules to remove the negative impacts of partial shade by nearly harmonising all modules' electrical characteristics. The DPP converters running the D-MPPT algorithm smoothed out the P-I characteristics of the mismatched PV string and eliminated the local maxima as shown in Figure 3.

As shown in Figure 3 elimination of local maximum power point (LMPP) eliminates the complicated MPPT for tracking maximum power under non-uniform irradiation.

Many authors have researched with variety of DC-DC converters such as fly-back, buck-boost, forward, switched inductor and capacitor networks, and so on [30–34]. These converters help to provide impedance matching at the sub-module level, thereby energy trapped is higher. Nevertheless, DPP converters are not connected to the same ground or common devices, so the structure of these DPP converter circuits is complex and requires more driving units with more powerful components. Additionally, as the total quantity of PV sub-modules rises, greater power loss results from the mismatched power having to go through multi-stage power conversion. It increases the cost and reduces the DPP conversion efficiency.

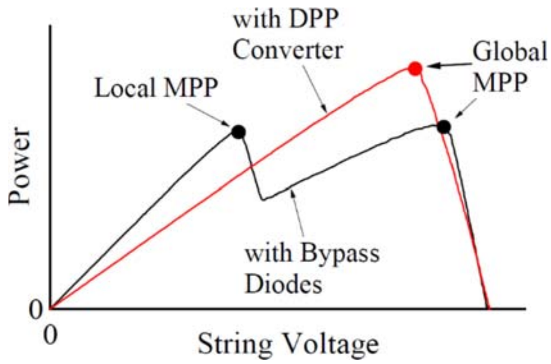

Fig. 3. P-V characteristics of string with bypass diodes and with DPP converter [34].

To overcome these drawbacks, this particular paper proposes a novel multi-port DC-DC converter to perform a distributed MPPT approach to trap the peak power of solar PV arrays. This system facilitates the direct transmission of mismatched power among non-adjacent sub-modules, thereby decreasing power loss and the number of conversion stages required to convert mismatched power. So, it minimizes number of components. Meantime peak power is tracked with smooth curve. Hence it is suitable for PV power plants which are implemented in wider areas where the possibility of partial shading is high. Employing DMPPT with the proposed converter reduces mismatch losses and complications in the control of power extraction.

Three modules have been considered to validate this proposed approach under dynamic cloud conditions. The multiple-peak tracking has been obtained using a multiport DC-DC converter. The mathematical modeling for solar PV with non-uniform cloud conditions are applied to examine the DMPPT approach in the proposed multiport converter. The operation details of the proposed converter along with analytical waveforms are presented. In addition, a detailed study on simulation exercises has been carried and the results are presented in this paper. Furthermore, the experimental prototype has been built to test in the real-time environmental and integrated with the solar PV system.

2 Mathematical Modeling of PV

For better understanding, the solar PV panel has been modeled with practical values in Power Systems Computer-Aided Design/Electromagnetic Transients including DC (PSCAD/EMDTC) software. The equivalent circuit of the single diode PV model along with the blocking diode is presented in Figure 4. It helps to investigate the shading effect and mismatch conditions under variable environmental conditions.

The PV generation current ($I_{\rm PV}$) can be expressed as,

$$I_{\rm PV} = \alpha I_{\rm SC0} - I_{\rm D0}\left(e^{\left(\frac{qU_{\rm PV}}{AKT}\right)} - 1\right) \tag{1}$$

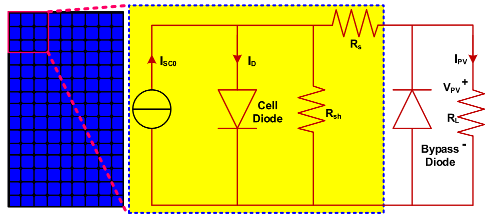

Fig. 4. Equivalent circuit of PV cell.

where, $V_{\rm PV}$ is the sub-module PV voltage and $I_{\rm SC0}$ is short-circuit current under standard conditions, $I_{\rm D0}$ is the saturation current, $U_{\rm PV}$ is the output voltage of the module, q is the charge of an electron, k is the Boltzmann constant, T is the temperature in Kelvin and A is the ideality factor. The mathematical expression of solar PV generated power $P_{\rm PV}$ can be written as,

$$P_{\rm PV} = V_{\rm PV}\left(\alpha I_{\rm SC0} - I_{\rm D0}\left(e^{\frac{qV_{\rm PV}}{AKT}}\right) - 1\right). \tag{2}$$

Similarly, the solar PV generated current and PV power with blocking diode can be written as,

$$I_{\rm PV} = \alpha I_{\rm SC0} - I_{\rm D0}\left(e^{\left(\frac{qV_{\rm PV}}{AKT}\right)} - 1\right) + I_{\rm S0}\left(e^{\left(-\frac{qV_{\rm PV}}{nKT}\right)} - 1\right) \tag{3}$$

$$P_{\rm PV} = V_{\rm PV}\left(\alpha I_{\rm SC0} - I_{\rm D0}\left(e^{\left(\frac{qV_{\rm PV}}{AKT}\right)} - 1\right) + I_{\rm S0}\left(e^{\left(-\frac{qV_{\rm PV}}{nKT}\right)} - 1\right)\right). \tag{4}$$

After DMPPT operation involves, the voltage gets adjusted based on algorithm, the final PV voltage appears at ith iteration as follows,

$$V_{{\rm PV}_i} = \frac{AKT}{q}\ln\left(1 + \frac{\alpha_i I_{\rm SC0} - I_{{\rm PV}_i}}{I_{\rm D0}}\right). \tag{5}$$

The above expression is true when all the sub-modules of PV voltage are equal. Similarly, based on the normalized irradiation factors $\alpha_1 = \alpha_2 = \alpha_3 = 1$ depending on the photo signal generated in sub-modules, the conditions for current can be expressed as,

$$\alpha_1 I_{\rm SC0} - I_{{\rm PV}_1} = \alpha_2 I_{\rm SC0} - I_{{\rm PV}_2} = \alpha_3 I_{\rm SC0} - I_{{\rm PV}_3}. \tag{6}$$

where $I_{{\rm PV}_1}$, $I_{{\rm PV}_2}$, $I_{{\rm PV}_3}$ subject to

$$\left\{\begin{array}{l} I_{{\rm PV}_1} = I_{{\rm DMP}_1} + I_{\rm PV} \\ I_{{\rm PV}_2} = I_{{\rm DMP}_1} + I_{{\rm DMP}_2} + I_{\rm PV} \\ I_{{\rm PV}_3} = I_{{\rm DMP}_1} + I_{{\rm DMP}_2} + I_{{\rm DMP}_3} + I_{\rm PV} \end{array}\right\}. \tag{7}$$

In order to satisfy expression (6), the proposed multiport DC-DC converter must adjust the duty cycle within the specified range. Therefore, the solar PV current and power of array can be written as,

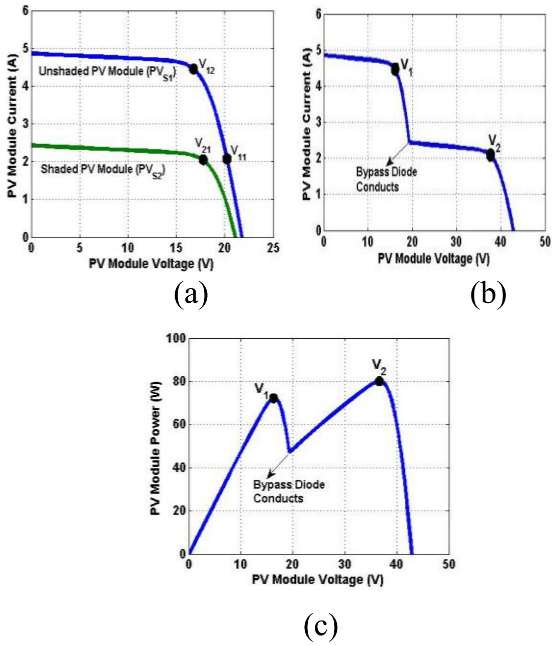

Fig. 5. PV module graphs under non-uniform irradiation. a) IV curve without by-pass diode; b) IV curve with by-pass diode; c) PV curve with by-pass diode.

$$I_{\mathrm{PV}} = \frac{1}{n}\sum_{i=1}^{n} I_{\mathrm{PV}_i}; n = 3 \tag{8}$$

$$\begin{aligned} P_{\mathrm{PV}} &= V_{\mathrm{PV}} I_{\mathrm{PV}} \\ &= V_{\mathrm{PV}}\left(\frac{\alpha_1+\alpha_2+\alpha_3}{3} I_{\mathrm{SC0}} - I_{\mathrm{D0}}\left(e^{\left(\frac{qV_{\mathrm{PV}}}{3AKT}\right)} - 1\right)\right). \end{aligned} \tag{9}$$

The same approach needs to be applied to all the sub-modules of an array to extract the maximum power under non-uniform irradiations across all the modules. Finally, the PV power under DMPPT operation can be determined as follows,

$$P_{\mathrm{mpp}} = V_{\mathrm{mpp}}\left(\frac{\alpha_1+\alpha_2+\alpha_3}{3} I_{\mathrm{SC0}} - I_{\mathrm{D0}}\left(e^{\left(\frac{qV_{\mathrm{smppi}}}{AKT}\right)} - 1\right)\right). \tag{10}$$

The depth analysis is made in the simulation platform after incorporating the necessary expressions. Thereby, the solar PV current and voltage at each module are mentioned in Figure 5. The shading factors are also adjusted and different irradiations are applied to each module for depth analysis. The IV and PV characteristics under non-uniform irradiation conditions are observed and plotted in Figure 5.

In Figure 5, V_{12} is the voltage of unshaded PV module, while V_{21} is the voltage of shaded PV module without by-pass diode. As shown in Figure 5, V_{21} is equal to V_{11} in an unshaded PV module which is lesser than $V_{12.}$ Under PSC with by-pass diode multiple peak voltages are produced as shown in Figure 5b which results local maximum peak power as depicted in Figure 5c.

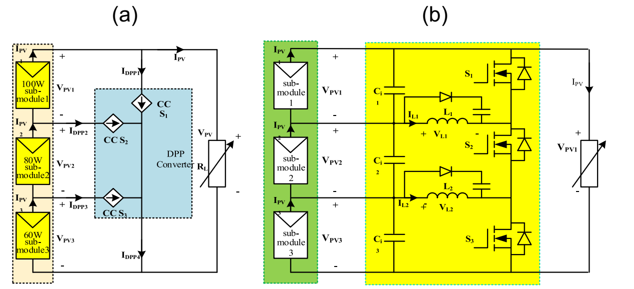

Fig. 6. Multi-port DC-DC converter. a) Structure of proposed converter; b) circuit diagram of proposed converter.

3 Proposed multiport DC-DC converter

The basic structure of the proposed novel multiport converter is presented in Figure 6a. The multiple variables to control the output voltage to perform MPPT operation are mentioned in Figure 6. The sub-modules of each solar panel can be controlled by an individual section of the multiport converter.

The circuit diagram of the proposed multi-port converter is presented in Figure 6b there are two passive elements (inductor and capacitor) that share their operation with two modules. Therefore, the number of components involved gets reduced, thereby enhancing the efficiency.

3.1 Mode 1

The circuit operation can be classified into two modes based ON and OFF states of the switch. Mode 1 as exhibited in Figure 7a: The switch S_1 is OFF state and the other two are off states. The inductors L_1, L_2 and Capacitors C_1, C_2 are charged and the inductor current gets raised due to this operation. During mode 1, the voltage expressions across the inductor can be written as,

$$V_{L_1} = L_1\frac{\mathrm{d}i_{L_1}}{\mathrm{d}t} + V_{C_1} = V_{\mathrm{pv}} \tag{11}$$

$$V_{L_2} = L_2\frac{\mathrm{d}i_{L_2}}{\mathrm{d}t} + V_{C2} = V_{\mathrm{pv}}. \tag{12}$$

During discharge mode, the inductor and capacitor energy together gets dissipated to the load via the anti-parallel diode of the switch. The current path is indicated in Figure 7a.

$$V_{L_1} = L_1\frac{\mathrm{d}i_{L1}}{\mathrm{d}t} = V_{\mathrm{pv}} - V_{C_1} \tag{13}$$

$$V_{L_2} = L_2\frac{\mathrm{d}i_{L2}}{\mathrm{d}t} = V_{C_1} + V_{\mathrm{o}}. \tag{14}$$

3.2 Mode 2 and 3

In mode 2, S_2 is off-condition and the current paths are clearly mentioned in Figure 7b similarly, in mode 3, the

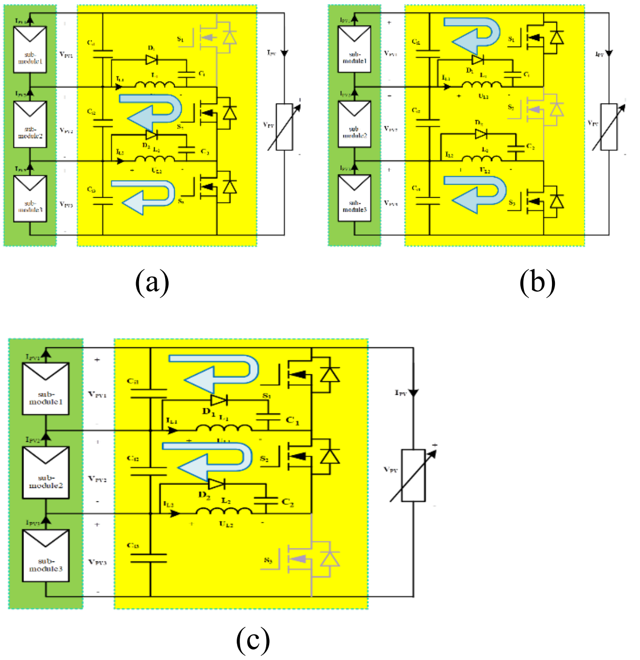

Fig. 7. Equivalent circuit of Multi-port DC-DC converter. a) Mode 1; b) Mode 2; c) Mode 3.

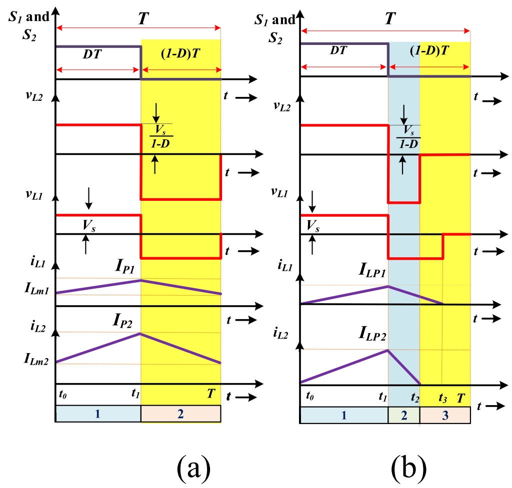

Fig. 8. Analytical waveform of multi-port DC-DC converter under a) CCM and b) DCM mode.

switch S_3 is in the off state as shown in Figure 7c. The mathematical expressions of these modes are also similar to mode 1. The operation details under modes 1, 2, and 3 are under continuous current mode (CCM) and discontinuous current mode (DCM) are clearly illustrated in Figure 8.

The voltage across the inductor and current through the capacitor becomes alternating quantity. As mentioned in the operation, the inductor current rising and the falling rate is plotted in proportion to the inductor voltage magnitude as well as polarity. The voltage across a capacitor can be written as,

$$V_{\mathrm{c}} = \frac{1}{1-D} V_{\mathrm{pv}}. \tag{15}$$

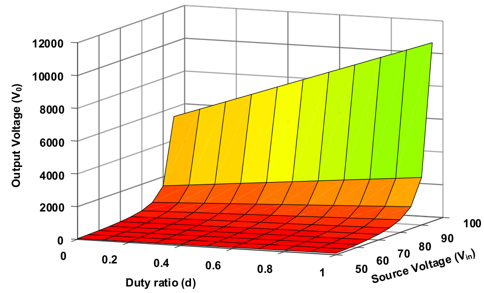

Fig. 9. Three-dimensional plot for output voltage with respect to duty cycle and PV voltage.

In equation (15), D is the duty ratio of the switching device. Based on the energy balance equation, the voltage that appears across the multi-port DC-DC converter can be determined by assuming the zero average voltage appears at the inductor to control the current through it.

$$V_{\mathrm{o}} = \frac{D V_{\mathrm{pv}} + V_{\mathrm{c_1}}}{1-D}. \tag{16}$$

Further, the output voltage can be written after applying capacitor voltage expressions in (16), the final expression becomes,

$$M = \frac{V_{\mathrm{o}}}{V_{\mathrm{pv}}} = \frac{1 + D - D^2}{(1-D)^2}. \tag{17}$$

Using (17), the peak gain value can be obtained at every change in the value of duty ratios and solar PV voltage and it has been plotted in three-dimensional pattern as shown in Figure 9. From this graph, the peak gain value can be chosen based on the duty cycle and PV voltage and is helpful to choose the suitable value of passive elements.

This article involves an examination of CCM because, for the same amount of output power, it reduces peak and average currents compared to DCM. In addition to maximising the switch's power capacity, this lowers dissipation and boosts efficiency.

4 Measured results and discussion

To test and validate the performance of the proposed multi-port DC-DC converter with the DMPPT approach, the investigation has been carried out in the simulation platform of PSCAD/EMDTC and results are presented. Three modules of less PV power are connected in a series structure with different cloud conditions as shown in Figure 10. The irregular irradiation is applied to all sub-modules and overall generation gets varied concerning environmental conditions. Module 1, 2 and 3 irradiations are set to be 600 W/m^2, 800 W/m^2 and 1000 W/m^2. It is indicated in Figure 10a. Cumulative generations of solar IV and PV characteristics are illustrated in Figures 10b and 10c.

After incorporating the perturb and observe (P&O) algorithm-based DMPPT operation, the instantaneous voltage and current of PV are generated at every sampling time. The reference voltage as a control parameter is

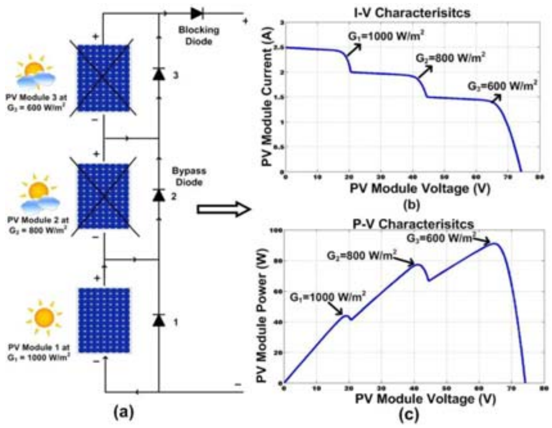

Fig. 10. Cumulative PV generation under non-uniform irradiations. a) Power generation via PV module, b) IV characteristics, c) PV characteristics.

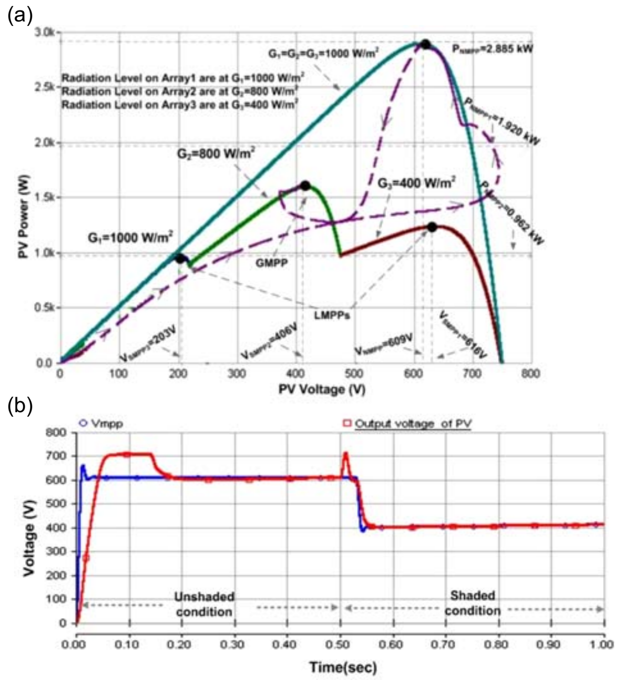

Fig. 11. Measured results of solar PV system with DMPPT approach using proposed multi-port DC-DC converter, a) P-V results b) V_{mpp} tracking with V_{pv} under all different irradiation levels.

identified by the algorithm based on the condition states of DMPPT. Thereafter, the closed-loop control mechanism helps to track the original MPP voltage of 66 V from the actual PV voltage. Thereby, the duty cycle is kept on adjusted at every sampling time. Finally, it achieves the DMP point to yield a maximum power of 90 W.

After implementing this DMPPT approach in the proposed multi-port DC-DC converter, the simulation results are observed as shown in Figure 11. The change in irradiation levels are applied as follows, $G_1 = 1000\ \mathrm{W/m^2}$, and another at radiation level of $G_2 = 800\ \mathrm{W/m^2}$ and of $G_3 = 400\ \mathrm{W/m^2}$ with shaded modules (Ns) $= 2$, and unshaded module (Ni) $= 1$. The voltage and current are adjusted according to changes in the duty cycle of each switch of the multi-port converter. The global MPPT or variable peak power is traced even with variable irradiation conditions.

For this, a PV array is formed with series connection of two arrays. Many modules are connected in series-parrallel combinations to form an array. By assuming the same operational conditions such as temprature, irradiations and efficiency levels for all the modules, the investigation is carried out. To identify the mismatch power operation, the above condition is considered. Now by setting the different irradiation levels at each PV array, the performance of the proposed system can be examined.

From the Figure 11, it is observed that under uniform irradiance PV power generated is 2.885 kw. Under the shaded condition, without the proposed system Global Maximum Power Point (GMPP) is 1550 W, whereas with the help of the proposed system PV power extracted is 1920 W. The proposed system extracts 370 W greater power than a conventional system. Figure 11b shows the effective tracking of maximum power point voltage (V_{mpp}) of PV by DMPPT as output voltage under both shaded and unshaded conditions. Tracking of voltage at the time of starting is 0.18 s by DMPPT while it is very less during change in irradiance condition as shown in Figure 11b.

The real-time implementaiton of the proposed multi-port DC-DC converter for DMPPT operation using the P&O method is shown in Figure 12. In order to verify the operation details of proposed multi-port DC-DC converter,

Fig. 12. Implementation of proposed multi-port DC-DC converter for DMPPT operation in real time solar PV plant.

the experimental results have been observed and presented for three panels in this section. Initially, the system is analysed under uniform irradiation conditions without any shading of any PV array, the inductor current of the proposed multiport converter and corresponding gating signals are presented in Figure 13a. The output voltage and input voltage along with inductor current waveforms of the multiport converter are captured in Figure 13b.

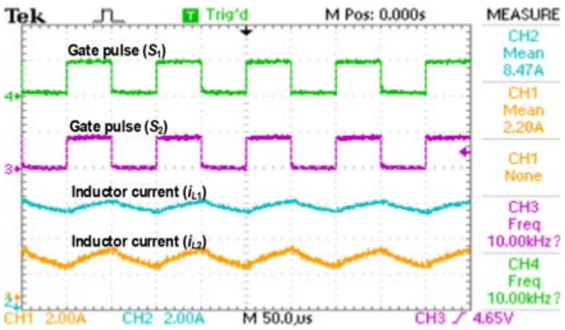

(a)

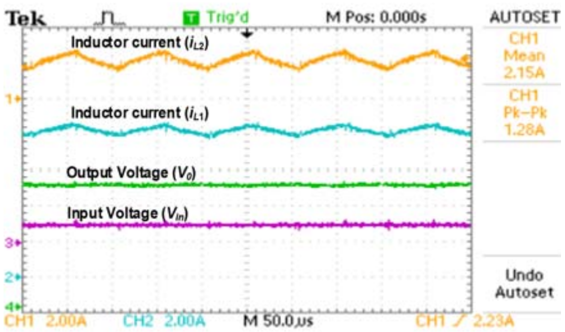

(b)

Fig. 13. Experimental results of multiport converter under fixed irradiations. a) Gating pulse and inductor currents, b) Input and output voltages.

From the Figure 13a it is observed that under non shaded condition duty cycles of S_1 and S_2 are same. The PV current is 8.47 A. The output voltage is constant and maintained at 149 V. PV power extracted in this condition is 1262 W. Similarly, under shaded irradiations on the PV arrays, similar to the simulation analysis one module is not shaded, other two modules are shaded manually. Voltage at input and output, voctage across inductor and capacitor of multiport converter are monitored. The PV peak power gets changed and different duty cycles are required in this proposed multi-port DC-DC converter.

The experimental results under this situation are observed and presented in Figure 14. This particular experimental result is shown in Figure 14a. The duty cycle of switching device S_1 is different from switching device S_2 since the operating point of DMPPT is different

The corresponding inductor current rising and falling are captured along with output and PV array voltages as shown in Figure 14b. From the Figure 14 it is observed that under shaded condition the PV current is 6.02 A. Output voltage is constant and maintained as 132 V. PV power extracted in this condtion is 795 W.

Simulation research shows that the suggested system extracts 24% (370 W) more power than the centralized converter and MPPT approach under shaded irradiance condition. In [35] DMPPT in series connected PV sub-modules with DPP under various shaded irradiance conditions. The DMPPT with a DPP-based PV system offered a

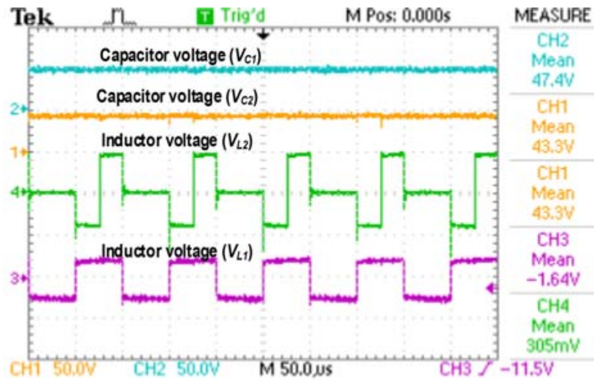

(a)

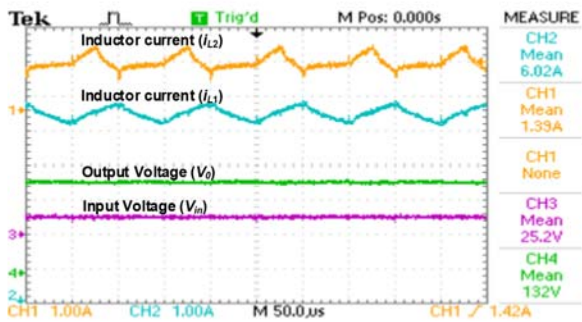

(b)

Fig. 14. Experimental results of multiport converter under variable irradiations. a) Capacitor and inductor voltages, b) Input and output voltages.

maximum improvement of 19.4% PV power extraction compared to those without a DPP system. Therefore, it is evident that the proposed multiport DC-DC converter is a more suitable converter to perform D-MPPT operation for solar PV power plants.

5 Conclusion

This paper aims to propose a highly efficient novel multi-port DC-DC converter to perform DMPPT operation when more modules are connected in an array. The modes of operation along with equivalent circuit and analytical waveforms are examined in this paper. The mathematical relations of PV voltage, current and multi-port DC-DC converter voltage and current concerning various parameters are derived and presented in the paper. In addition, the simulation study has been done under on-uniform irradiations for each PV array and the results have been discussed in the paper. According to the simulation analysis, the suggested system demonstrates a 24% enhancement in power extraction when compared to the centralised converter and MPPT approach, particularly in the presence of shadowed irradiance. The proposed multi-port DC-DC converter has been implemented experimentally to test its feasibility in a real-time environment and measured results are presented. After a detailed investigation and discussion of measured results and analysis, it is concluded that the proposed multi-port DC-DC converter is the most suitable solution for solar PV applications. In this article analysis of the proposed system is verified with three sub-modules of PV array, in future research may extend to real-time wide power plant with multi rows and columns of PV array to validate the efficacy of DMPPT and proposed multi-port DC-DC converter.

References

1 Fikri E., Sulistiawan I.A., Riyanto A., Saputra A.E. (2023) Neutralization of acidity (pH) and reduction of total suspended solids (TSS) by solar-powered electrocoagulation system, *Civ. Eng. J.* **9**, 5, 1160–1172.

2 Bedewy B.A.H., Al-Timimy S.R.A. (2023) Estimate suitable location of solar power plants distribution by GIS spatial analysis, *Civ. Eng. J.* **9**, 5, 1217–1229.

3 Krishna B., Karthikeyan V. (2021) Ultra-voltage gain step-up DC-DC converter for renewable energy micro-source applications, *IEEE Trans. Energy Convers.* **37**, 2, 947–957.

4 Kabir E., Kumar P., Kumar S., Adelodun A.A., Kim K.H. (2018) Solar energy: potential and future prospects, *Renew. Sustain. Energy Rev.* **82**, 894–900.

5 Phani Kumar Ch, Elanchezhian E.B., Pragaspathy S. (2022) An adaptive regulatory approach to improve the power quality in solar PV-integrated low-voltage utility grid, *J. Circuits Syst. Comput.* **31**, 17, 2250301.

6 Balal A., Jafarabadi Y.P., Demir A., Igene M., Giesselmann M., Bayne S. (2023) Forecasting solar power generation utilizing machine learning models in Lubbock, *Emerg. Sci. J.* **7**, 4, 1052–1062.

7 Hole S.R., Goswami A.D. (2022) Maintain maximum power point tracking of photovoltaic using SEPIC converter, In: *2022 2nd International Conference on Power Electronics & IoT Applications in Renewable Energy and its Control (PARC)*, IEEE, pp. 1–6.

8 Hole S.R., Goswami A.D. (2024) Design of a novel hybrid soft computing model for passive components selection in multiple load Zeta converter topologies of solar PV energy system, *Energy Harvesting Syst.* **11**, 1, 20230029.

9 Hole S.R., Goswami A.D. (2022) Quantitative analysis of DC–DC converter models: a statistical perspective based on solar photovoltaic power storage, *Energy Harvesting Syst.* **9**, 1, 113–121.

10 Hole S.R., Goswami A.D. (2023) Design of an efficient MPPT optimization model via accurate shadow detection for solar photovoltaic, *Energy Harvesting and Syst.* **10**, 2, 377–383.

11 Hole S.R., Goswami A.D. (2022) Analysis and performance of solar photovoltaic energy system in India: case study, in: *2022 4th International Conference on Inventive Research in Computing Applications (ICIRCA)*, IEEE, pp. 228–234.

12 Qi J., Zhang Y., Chen Y. (2014) Modeling and maximum power point tracking (MPPT) method for PV array under partial shade conditions, *Renew. Energy* **66**, 337–345.

13 Olabi A.G., Abdelkareem M.A., Semeraro C., Al Radi M., Rezk H., Muhaisen O., Al-Isawi O.A., Sayed E.T. (2023) Artificial neural networks applications in partially shaded PV systems, *Therm. Sci. Eng. Prog.* **37**, 101612.

14 Ragb O., Bakr H. (2023) A new technique for estimation of photovoltaic system and tracking power peaks of PV array under partial shading, *Energy* **268**, 126680.

15 Alghamdi A.S., Bahaj A.S., Blunden L.S., Wu Y. (2019) Dust removal from solar PV modules by automated cleaning systems, *Energies* **12**, 15, 2923.

16 Bhatt P.K., Kumar S.Y. (2018) Investigations on operational characteristics of a PV integrated unbalance distribution system for energy management studies, *Curr. Altern. Energy* **2**, 1, 72–80.

17 Green M.A., Emery K., Hishikawa Y., Warta W., Dunlop E.D. (2022) Solar cell efficiency tables (Version 48), *Prog. Photovolt. Res. Appl.* **30**, 3–13. https://aurorasolar.com/blog/shading-losses-in-pv-systems-and-techniques-to-mitigate-them/

18 Jain S., Sharma T., Gupta A.K. (2022) End-of-life management of solar PV waste in India: Situation analysis and proposed policy framework, *Renew. Sustain. Energy Rev.* **153**, 111774.

19 Tripathi A.K., Aruna M., Murthy C.S. (2019) Output power enhancement of solar PV panel using solar tracking system, *Recent Adv. Electr. Electron. Eng.* **12**, 1, 45–49.

20 Park C., Jeong B., Zhou P., Jang H., Kim S., Jeon H., Nam D., Rashedi A. (2022) Live-Life cycle assessment of the electric propulsion ship using solar PV, *Appl. Energy* **309**, 118477.

21 Mohapatra A., Nayak B., Das P., Mohanty K.B. (2017) A review on MPPT techniques of PV system under partial shading condition, *Renew. Sustain. Energy Rev.* **80**, 854–867.

22 Bingöl O., Özkaya B. (2018) Analysis and comparison of different PV array configurations under partial shading conditions, *Solar Energy* **160**, 336–343.

23 Pawluk R.E., Chen Y., She Y. (2019) Photovoltaic electricity generation loss due to snow – A literature review on influence factors, estimation, and mitigation, *Renew. Sustain. Energy Rev.* **107**, 171–182.

24 Zhang W., Liu S., Gandhi O., Rodríguez-Gallegos C.D., Quan H., Srinivasan D. (2021) Deep-learning-based probabilistic estimation of solar PV soiling loss, *IEEE Trans. Sustain. Energy* **12**, 4, 2436–2444.

25 Lakshika K.H., Boralessa M.K.S., Perera M.K., Wadduwage D.P., Saravanan V., Hemapala K.M.U. (2020) Reconfigurable solar photovoltaic systems: A review, *Heliyon* **6**, 11, e05530.

26 Venkatramanan D., John V. (2019) A reconfigurable solar photovoltaic grid-tied inverter architecture for enhanced energy access in backup power applications, *IEEE Trans. Ind. Electron* **67**, 12, 10531–10541.

27 Krishna B., Uma Maheswar Rao P., Karthikeyan V. (2022) High-gain single-switch single-input dual-output DC-DC converter with reduced switching stress, *Int. J. Circuit Theory Appl.* **50**, 6, 1998–2015.

28 López-Erauskin R., Gonzalez A., Petrone G., Spagnuolo G., Gyselinck J. (2020) Multi-variable perturb and observe algorithm for grid-tied PV systems with joint central and distributed MPPT configuration, *IEEE Trans. Sustain. Energy* **12**, 1, 360–367.

29 Alonso R., Ibáñez P., Martinez V., Román E., Sanz A. (2010) Analysis of performance of new distributed MPPT architectures, in: *2010 IEEE International Symposium on Industrial Electronics*, IEEE, pp. 3450–3455.

30 Bhatt P.K., Kumar S.Y. (2017) Filtering scheme to mitigate the harmonic issues in solar PV integrated nonlinear distribution system, *Recent Adv. Electr. Electron. Eng.* **1**, 1, 44–52.

31 Chao Y., Chen C., Chang L. (2014) Distributed maximum power point tracking for photovoltaic systems, *IEEE Trans. Ind. Electron.*, **61**, 4, 1830–1842.

32 Sharma R., Kumar V., Sharma S., Karthikeyan V., Kumaravel S. (2018) High efficient solar PV fed grid connected system, in: *2018 IEEE International Conference on Power Electronics, Drives and Energy Systems (PEDES)*, IEEE, pp. 1–6.

33 Zhang T., Jiang J., Chen D. (2021) An efficient and low-cost DMPPT approach for photovoltaic submodule based on multi-port DC converter, *Renew. Energy* **178**, 1144–1155.

34 Uno M., Shinohara T., Saito Y., Kukita A. (2019) Review, comparison, and proposal for PWM converters integrating differential power processing converter for small exploration rovers, *Energies* **12**, 10, 1919.

35 Bell R., Pilawa-Podgurski R.C. (2015) Decoupled and distributed maximum power point tracking of series-connected photovoltaic submodules using differential power processing, *IEEE J. Emerg. Sel. Top. Power Electron.* **3**, 4, 881–891.